Frequency-domain Constructed Redundant Bases for Denoising

Jianyu Lin
The Brain & Mind Research Institute
The University of Sydney
NSW 2006, Australia

Graham C. Goodwin
School of Electrical Eng. & Computer Science
University of Newcastle
Callaghan, NSW 2308, Australia

Abstract – In this paper, redundant bases for denoising are constructed completely in the frequency-domain. The advantage of the frequency-domain bases construction approach is that it provides much more flexibility. As a result, the filterbank (basis) can be constructed to fit the features of the signal more closely, and the filter's frequency response in the filterbank can be designed to be very close to the Gaussian curve so that the time-frequency localization is close to optimal. Experimental results show that the new bases perform very well with signals that can be very difficult for denoising with conventional bases, such as conventional wavelets, wavelet packets, and wavelet frames etc.

Key words – denoising, redundant basis, wavelets, wavelet frames

1 Introduction

Wavelet frames is known to perform better than wavelets and wavelet packets for denoising task [1-5]. There have been some direct applications of the wavelet frame denoising technique recently [7],[8]. The reason that wavelet frames performs better for denoising is that the basis for wavelet frames is redundant. Redundancy can exist in both time and frequency domain, or only the time domain. For example, filtering with Haar filters without down sampling generates redundancy in the time domain, but there is no redundancy in the frequency domain. Using higher order spline filters, there will be redundancy in both frequency and time domain [2]. Here is an example of the spline tight frames whose FIR filters coefficients are shown below:

h1 = {0.0625, 0.2500, 0.3750, 0.2500, 0.0625}
h2 = {-0.1250, -0.2500, 0, 0.2500, 0.1250}
h3 = {-0.1531, 0, 0.3062, 0, -0.1531}
h4 = {0.1250, -0.2500, 0, 0.2500, -0.1250}
h5 = {0.0625, -0.2500, 0.3750, -0.2500, 0.0625}

Since these FIR filters must satisfy certain conditions to form a tight frame, the bandwidths and the shapes of the filters' frequency responses cannot be modified arbitrarily. In other words, only iterative decompositions are allowed. For example, the Haar filters (for the Haar frames) consist of only two filters – low and high. Every iteration of filtering splits one band into two bands. The decomposition is the same as orthogonal decomposition except there is no down sampling so that there are redundancies in the time domain. There is no room to modify anything in the frequency domain – even redundancy cannot be introduced in the frequency domain. For spline filters, although there are redundancies in the frequency domain, the decomposition is still restricted to be iterative. Again, the final bandwidths and the final frequency response shapes of the filters in the filterbank cannot be arbitrarily modified.

In this paper, we propose a method for constructing redundant basis in the frequency domain. The advantage of the new method is the flexibility for bandwidth and the filter frequency response shape of the filterbank. With such flexibility, we are able to achieve better time-frequency localization of the bases so that sparser decomposed coefficients can be obtained. Consequently, better denoising results are expected.

2 Generalization of the Haar Frame

Figure 1 shows a signal called "Piece-Polynomial" that is widely used for testing denoising algorithms. It turns out that the simple Haar frame formed by omitting down sampling in the orthogonal decomposition is very effective for denoising signals with sharp edges, such as the Piece-Polynomial signal.

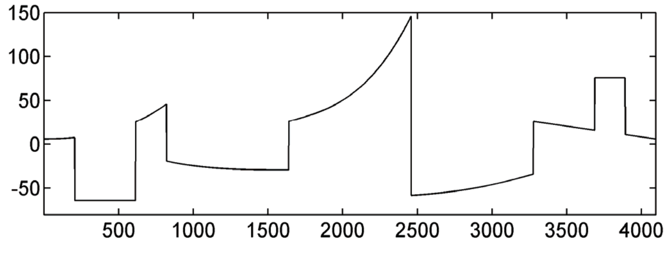

Fig 1. "Piece-Polynomial" signal

The bandwidths for the Haar frame coefficients are sketched in figure 2a. It is obvious that there is no redundancy in the frequency domain. If we can add in redundancy in the frequency domain such as the extra bands sketched by dashed lines in figure 2b, we would expect a higher performance than the original Haar frame. However, with the original scheme of performing Haar filtering using FIRs in the time domain, this is impossible. In other words, a precise Haar frame cannot generate redundancy in the frequency domain as sketched in figure 2b. However, if we consider the filtering process in the frequency domain, we can easily generate the redundancies shown in figure 2b while keeping the basis very close to Haar basis.

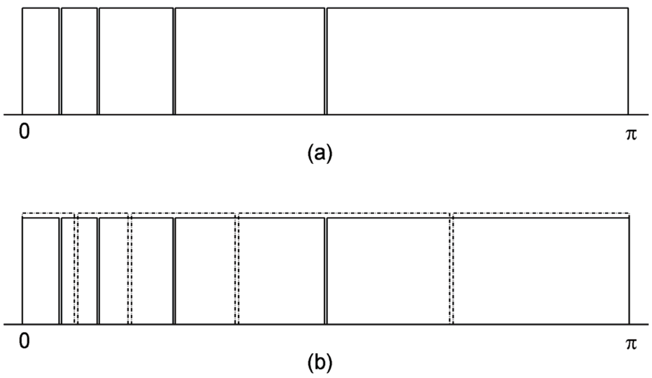

Fig 2. (a) Sketch of the bands produced by Haar basis. There is no redundancy in the frequency domain. (b) Extra bands shown in dashed line are added to bands in (a) so that redundancy in the frequency domain is introduced.

Consider decomposition and reconstruction of the Haar frame in the frequency domain. The frequency responses of the Haar filters are

$$\begin{cases} H_1(\omega) = \cos(\omega/2) \\ G_1(\omega) = \sin(\omega/2) \end{cases} \tag{1}$$

where $H_1(\omega)$ is the frequency response for the low-pass filter and $G_1(\omega)$ is for the high-pass filter. It is not difficult to see that for the second level decomposition

$$\begin{cases} H_2(\omega) = \cos(\omega) \\ G_2(\omega) = \sin(\omega) \end{cases} . \tag{2}$$

The frequency responses of filters for higher levels $H_n(\omega)$ $G_n(\omega)$ for n>2 can be found similarly.

Consider a 2-level decomposition in the frequency domain. After decomposition there are 3 bands. Suppose signal a_i (i=0, 1, 2, …, N-1) to be decomposed is of finite length N. Let A_i be the DCT coefficients of the signal a_i (DCT is used to avoid the discontinuity at the ending points). It can be shown that the spectra for the 3 bands are:

$$\begin{cases} B_{0i} = H_2(\pi\, n/N)H_1(\pi\, n/N)A_i \\ B_{1i} = G_2(\pi\, n/N)H_1(\pi\, n/N)A_i \\ B_{2i} = G_1(\pi\, n/N)A_i \end{cases} \tag{3}$$

Now let

$$\begin{cases} F_0(\omega) = H_2(\omega)H_1(\omega) \\ F_1(\omega) = G_2(\omega)H_1(\omega) \\ F_2(\omega) = G_1(\omega) \end{cases} \tag{4}$$

then,

$$\begin{cases} B_{0i} = F_0(\pi\, n/N)A_i \\ B_{1i} = F_1(\pi\, n/N)A_i \\ B_{2i} = F_2(\pi\, n/N)A_i \end{cases} \tag{5}$$

The decomposed coefficients, i.e. the outputs of the three bands from the filters can be found by the inverse DCT of B_{0i}, B_{1i}, B_{2i}. This is decomposition in the frequency domain.

For reconstruction,

$$A_i = F_0(\pi\, n/N)B_{0i} + F_1(\pi\, n/N)B_{1i} + F_2(\pi\, n/N)B_{2i} \tag{6}$$

This is because

$$[F_0(\omega)]^2 + [F_1(\omega)]^2 + [F_2(\omega)]^2 = 1 \qquad (0 \le \omega \le \pi) \tag{7}$$

Once A_i is known, a_i is simply the inverse DCT of A_i. For N-level decomposition, there will be N+1 bands, and it is not difficult to see that

$$\begin{cases} F_0(\omega) = H_N(\omega)H_{N-1}(\omega)\ldots H_1(\omega) \\ F_1(\omega) = G_N(\omega)H_{N-1}(\omega)\ldots H_1(\omega) \\ F_2(\omega) = G_{N-1}(\omega)H_{N-2}(\omega)\ldots H_1(\omega) \\ \quad \ldots\ldots \\ F_N(\omega) = G_1(\omega) \end{cases} \tag{8}$$

and

$$[F_0(\omega)]^2 + [F_1(\omega)]^2 + \ldots + [F_N(\omega)]^2 = 1 \qquad (0 \le \omega \le \pi) \tag{9}$$

The decomposition and reconstruction procedures are similar to the two-level case.

From the decomposition and reconstruction procedures, we are able to find the flexibility in constructing redundant basis in the frequency domain for periodic signals. (Note, when DCT is performed for the finite signal, the signal is symmetrically and periodically extended. The restriction of periodic signal here is not a strong one for applications, because we can always cut a long signal into pieces, and then extend them by DCT.) All we need is to find a filterbank, $F_0(\omega)$, $F_1(\omega)$, …, $F_N(\omega)$ such that equation

(9) is satisfied.

Return to the problem of introducing redundancy in the frequency domain for the Haar basis. Suppose $F_0(\omega)$, $F_1(\omega)$, …, $F_N(\omega)$ are the band-pass filters for an N-level Haar basis obtained from (8), and suppose their bandwidths are described by figure 2a. Let

$$F_i'(\omega) = F_i(\omega/\sqrt{2}) \qquad (10)$$

Obviously,

$$[F_0'(\omega)]^2 + [F_1'(\omega)]^2 + ... + [F_N'(\omega)]^2 = 1 \quad (0 \le \omega \le \pi) \qquad (11)$$

and the bandwidths of filters $F_i'(\omega)$ are the bands sketched with dashed lines in figure 2b. Now, consider the filterbank $F_0(\omega)$, $F_0'(\omega)$, $F_1(\omega)$, $F_1'(\omega)$, … $F_N(\omega)$, $F_N'(\omega)$. We have,

$$[F_0(\omega)]^2 + [F_0'(\omega)]^2 + [F_1(\omega)]^2 + [F_1'(\omega)]^2 + \\ ... + [F_N(\omega)]^2 + [F_N'(\omega)]^2 = 2 \\ (0 \le \omega \le \pi) \qquad (12)$$

With a simple normalization of the filters, we have

$$[F_0(\omega)]^2 + [F_0'(\omega)]^2 + [F_1(\omega)]^2 + [F_1'(\omega)]^2 + \\ ... + [F_N(\omega)]^2 + [F_N'(\omega)]^2 = 1 \\ (0 \le \omega \le \pi) \qquad (13)$$

This way, the redundancy in the frequency domain is introduced. Although the basis introduced by $F_i'(\omega)$ is not exactly the Haar basis, yet it is very close to the Haar basis (which can be seen easily by plotting of the basis).

We have tested this generalized redundant Haar Basis. The noisy signal is produced by adding Gaussian noise to the Piece-Polynomial signal shown in figure 1. The SNR used was 8 dB. For 1000 trials, the average SNR after denoising using the simple redundant Haar basis (i.e. without frequency redundancy) was 24.83 dB. The average SNR for the generalized redundant Haar basis (i.e. with our method of introducing frequency redundancy) was 25.05 dB. Although the improvement is not very large, it is very robust in the sense that statistically for more than 9 out of 10 trials (908 trials out of 1000 trials) the generalized redundant Haar basis produces higher SNR result than the original redundant Haar basis.

3 Modified Gaussian-shaped filterbank redundant basis

The introduction of frequency redundancy for Haar basis is used as an example to show that decomposition in the frequency domain is more flexible. The flexibility comes from the less restrictive requirement (9). As a matter of fact, there is more to be done with (9).

Firstly, let us look at the flexibility for the bandwidth of the filterbank. It is true that the Haar basis performs very well for signals with sharp edges such as the "Piece-Polynomial" shown in figure 1. However, it does not work well for signals that are more localized in the frequency domain, such as a complex tone with harmonics. Such features are very common in audio signals. For such kinds of signals, narrow bandwidth filters are required. Haar filters are well localized in the time domain and thus very poorly localized in the frequency domain. Higher order spline filters (such as the one shown in the introduction) have narrower bandwidths, yet the relationship between the bandwidths and the center frequencies is not flexible enough so that one can arbitrarily generate a specified bandwidth – center frequency relation so as to fit some existing model, for example, the critical band of an auditory system. As shown later, such a requirement can be easily satisfied if we take advantage of the flexibility from (9).

Secondly, as is known, when the frequency response of a filter is a Gaussian curve, localization of the filter in both time and frequency domain as a whole is optimal. Unfortunately, such filters cannot be used to construct tight frames. However, we will take advantage of (9) to construct filters whose frequency response is close (actually very close) to the Gaussian curve to achieve the best localization of the basis in both time and frequency domain, and at the same time they are tight frames except that their support is infinite (in the time domain).

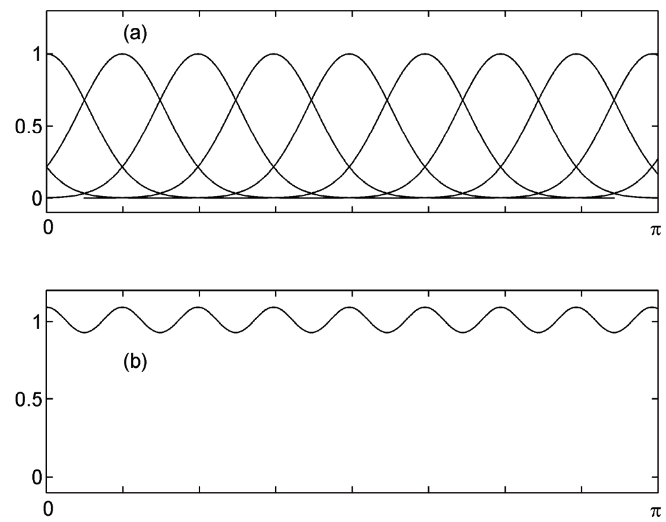

Fig 3. Frequency response of the filterbank (see text)

We start from computing the bandwidth b of the Gaussian curve. Let $\exp(-\omega_c^2/\sigma^2) = 1/\sqrt{2}$ (i.e. the position of -3 dB drop), then $\omega_c = 0.59\sigma$, thus the bandwidth $b = 2\omega_c$. Notice that the support for the

Gaussian curve is infinite. In reality, a chopped curve should be good enough. Suppose the curve is chopped at $\omega = \omega_0$ (of course $\omega_0 >> \omega_c$), then the final frequency response is taken as

$$H(\omega) = \begin{cases} \exp(-\frac{\omega^2}{\sigma^2}) - \exp(-\frac{\omega_0^{\ 2}}{\sigma^2}) & (-\omega_0 \le \omega \le \omega_0) \\ 0 & \text{otherwise} \end{cases} \tag{14}$$

(14) is used to guarantee that the curve is continuous at the chopping point.

Next, let us show how to obtain $F_i(\omega)$ from the $H(\omega)$ given by (14) so as to satisfy (9). As a matter of fact, for any arbitrary filter, as long as the redundancy in the frequency domain is high enough, (9) is approximated very well [2], [6]. Of course, this can also be seen using the Gaussian curve. The simplest condition is that all the responses have the same bandwidth, i.e. $F_i(\omega) = H(\omega)$ for all i, which is plotted in figure 3. In figure 3a, responses of all the filters in the filterbank are plotted. The distance in between any two adjacent filters is chosen to be half of the bandwidth $d = b/2$. In figure 3b, the sum

$$R(\omega) = \sum F_i^2(\omega) \tag{15}$$

for $F_i(\omega)$ in figure 3a is plotted. If the sum is an exact constant, (9) is satisfied by a simple normalization. As can be seen from figure 3b, the sum is quite close to a constant. As a matter of fact, if we change the distance among the filters' response to a quarter of the bandwidth $d = b/4$, the sum becomes even closer to constant, which is shown in figure 4 (in this case, only by changing the scale of graph for figure 4b, can the ripples in $R(\omega)$ be seen). In fact, if we choose d small enough, $H(\omega)$ can be used directly as an approximation of $F_i(\omega)$. However, we want perfect reconstruction, not approximations. This is very easy to do. Simply normalize $F_i(\omega)$ such that

$$F_i'(\omega) = F_i(\omega) \Big/ \sqrt{R(\omega)} \tag{16}$$

It is easy to see that $F_i'(\omega)$ satisfies (9) exactly. Thus perfect reconstruction for decomposition on redundant basis from $F_i'(\omega)$ is possible using the frequency domain decomposition method discussed earlier (it actually is a tight frame, but the support is infinite).

It is important to observe that since $R(\omega)$ is very close to a constant, $F_i'(\omega)$ is very close to Gaussian. Therefore, the redundant basis produced by the filterbank $F_i'(\omega)$ is more time-frequency localized than bases produced by other filterbanks.

Having shown the case where all of the filters in the filterbank have the same bandwidth, there is no difficulty in generalizing the case to filterbanks whose bandwidths are given as a function of the center frequencies.

Finally, we tested the modified Gaussian-shaped filterbank redundant basis described above on denoising a linear chirp signal corrupted by the Gaussian random noise.

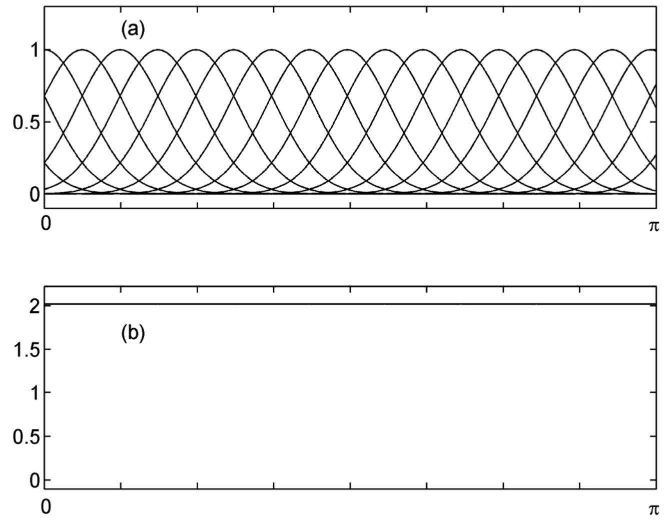

Fig 4. Frequency response of the filterbank (see text)

As shown in Figure 5: 5a is the original signal, and 5b shows the corrupted signal. The SNR of the corrupted signal is 6 dB. 5c is obtained using the Gaussian-shaped filterbank redundant basis. Constant bandwidth of the filterbank is chosen, i.e. the bandwidth does not increase as the center frequency of the filters in the filterbank increases. It achieves the highest signal to noise ratio among all the methods used, 17.31dB. Next, the denoised signal using wavelet packet is plotted in Figure 5d. It achieves 9.10 dB SNR. The result is obtained using the exiting command in Matlab:

```
xwpd=wpdencmp(cs,'h',4,'sym8','threshold',thr,1);
```

The third method is the spline tight frames whose FIR filters coefficients are shown in the introduction. The denoised signal is plotted in figure 5e, and the SNR is 8.10 dB. The last method is the dyadic wavelet denoising, using the existing command in Matlab:

```
xwd=wden(cs,'rigrsure','h','sln',5,'sym8');
```

The denoised signal is plotted in Figure 5f, and the SNR is 6.24 dB – extremely poor performance.

The results show that the existing denoising methods do not work very well for the oscillatory signals, i.e. signals that are well localized in the frequency domain. The new method of using the Gaussian-shaped filterbank redundant basis achieves substantial improvement for such signals. This is because the designed filterbank fits the signal's feature very well. It is important to mention that since the new method has high flexibility in designing the filterbanks, the filterbanks can be designed for different types of signals (not restricted to frequency-domain localized signals as the one used in our experiment).

4 Conclusion

Redundant basis for denoising is constructed completely in the frequency-domain. The advantage of constructing bases in the frequency domain is that much more flexibility is achieved, and thus the filterbank (basis) can be constructed to fit the features of the signal more closely. As a result, much better denoising results are expected for some difficult signals such as those that are localized well in the frequency domain. At the same time, for signals that can be denoised well with the conventional methods (bases), the new method also works well without any compromise.

References

[1] S. Qian and D. Chen, *Time-Frequency Analysis, Englewood Cliffs*, NJ: Pretice-Hall, 1996.

[2] S. Mallat, *A Wavelet Tour of Signal Processing*, Boston MA: Academic, 1998.

[3] D. L. Donoho and I. M. Johnstone, "Ideal spatial adaptation by wavelet shrinkage," *Biometrika*, vol.81, no.3, 425-455, 1994.

[4] D. L. Donoho, "De-noising by soft-thresholding," *IEEE Trans. Inform. Theory*, vol.41, no.3, 613-627, 1995.

[5] D. L. Donoho and I. M. Johnstone, "Adapting to unknown smoothness via wavelet shrinkage," *J. Amer. Stat. Assoc.*, vol.90, no.432, 1200-1224, 1995.

[6] I. Daubechies, *Ten Lectures on Wavelets,* Capital City Press, Montpelier, Vermont, 1992

[7] Y. Zhang, Y. Wang and W. Wang, "Denoising quadrature Doppler signals from bi-directional flow using the wavelet frame," *IEEE Trans. Ultra. Ferro. Freq. Contr.*, Vol 50, Iss. 5, 561 – 564, May 2003

[8] L.A. Kakadiaris, et al. "Surface denoising using a tight frame," *Pro. Computer Graphics International, 2004.*

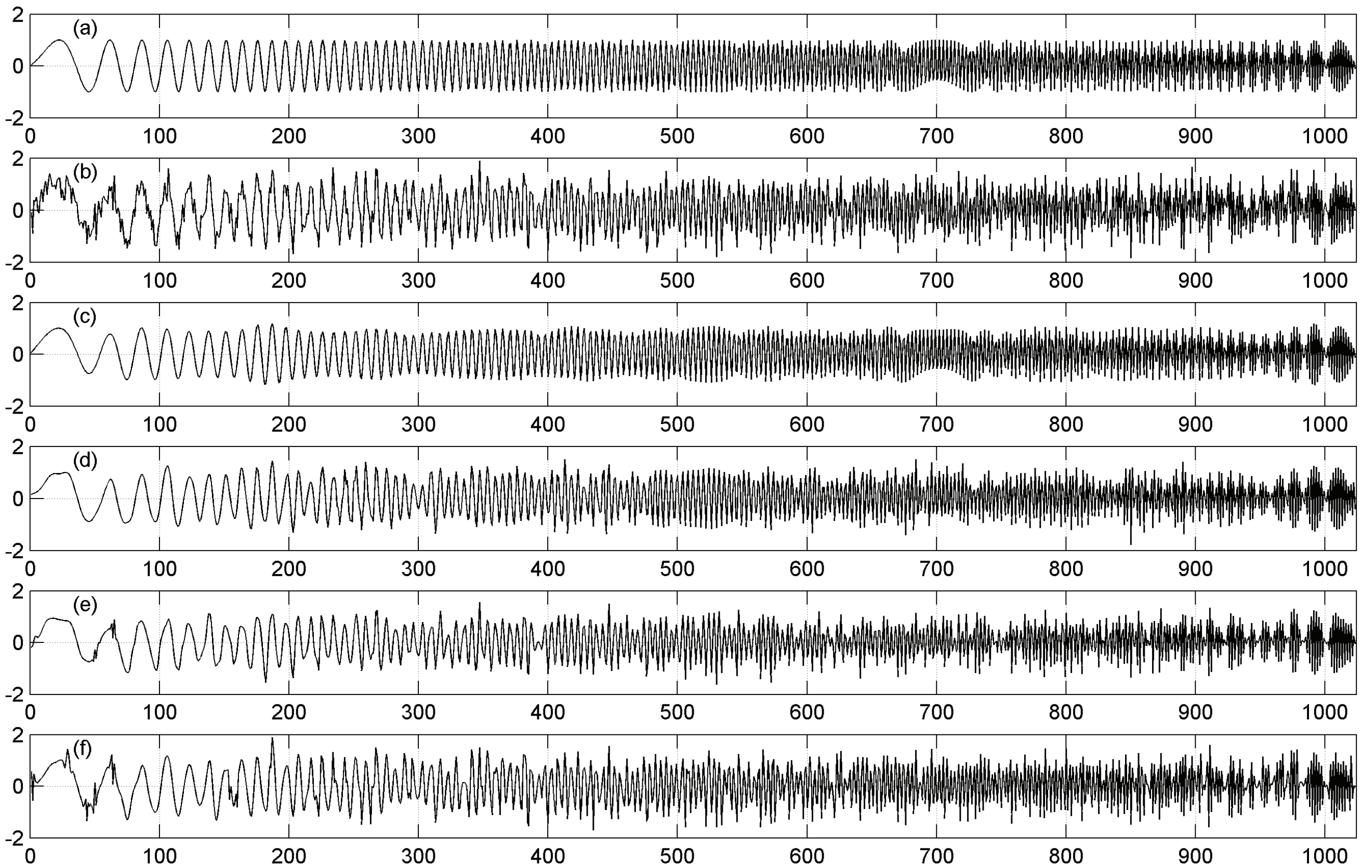

Fig 5. Experiment 1 – linear chirp denoising